Graphical Abstract

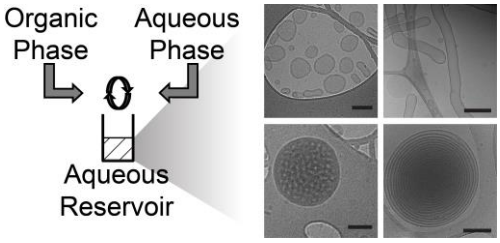

Figures

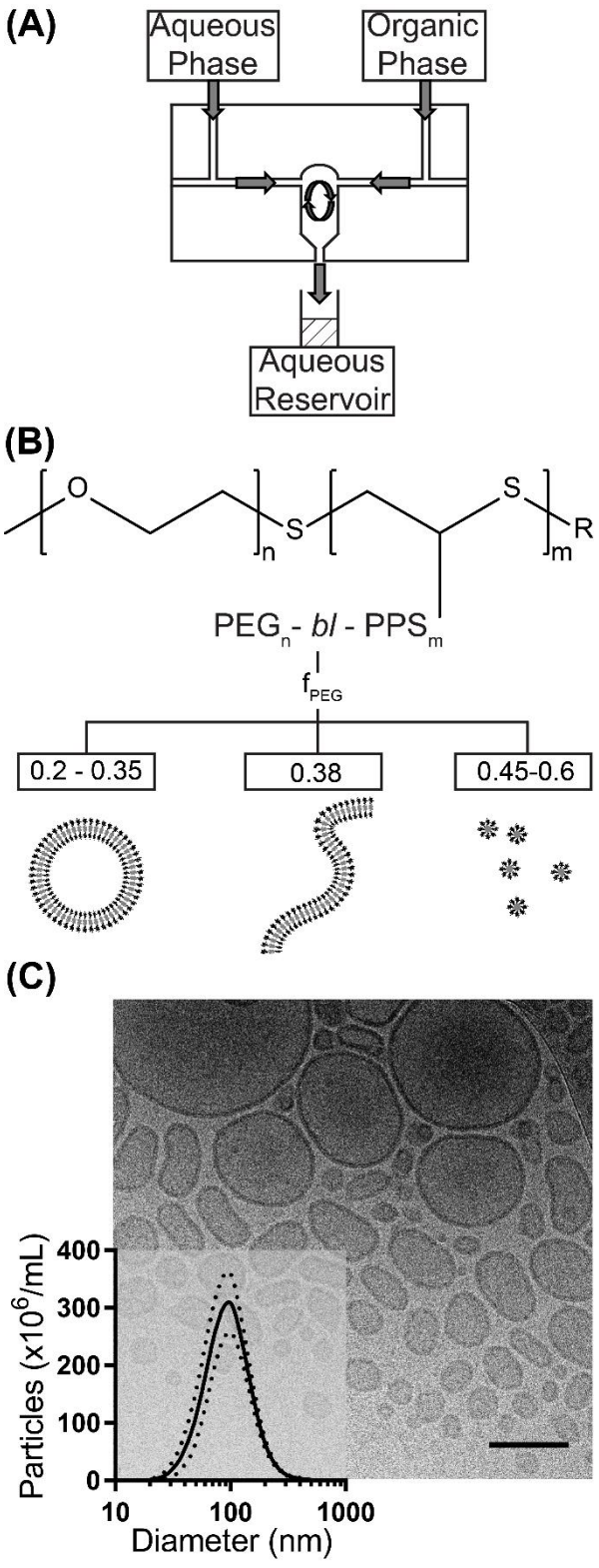

Fig. 1. Overview of polymersome formation by flash nanoprecipitation (FNP). (A) A schematic of the CIJ mixer. (B) The structure of the diblock copolymer poly(ethylene glycol)-*block*-poly(propylene sulfide), and the weight fraction (f_{PEG}) dependent nanostructures known to form using the thin film hydration method. (C) A representative cryoTEM image of polymersomes formed by FNP, scale bar = 300 nm. Inset is a size distribution of polymersomes measured by nanoparticle tracking analysis (NTA), n = 6. Standard deviation is represented by the dotted lines.

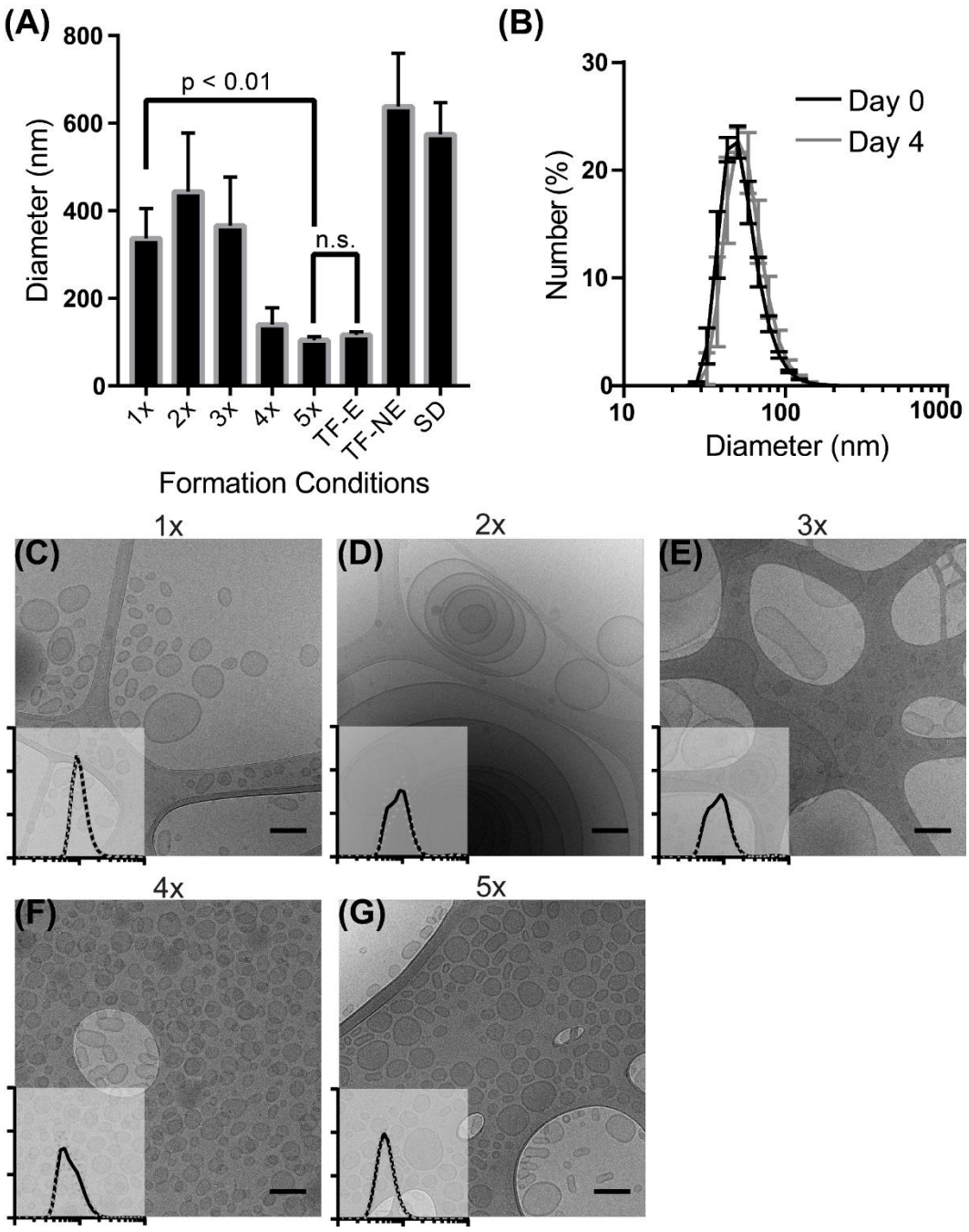

Fig. 2. Fabrication of monodisperse polymersomes via flash nanoprecipitation. (A) DLS mean diameter of polymersomes formed after multiple impingements (1x-5x), or formed by thin film (TF) or solvent dispersion (SD) with (E) or without (NE) extrusion. Error bars are standard error, n = 5. (B) DLS size distribution of 5x impinged polymersomes the day of formation or after four days of storage at room temperature. Error bars are standard error, n = 3. (C-G) CryoTEM images of polymersomes formed after multiple impingements (1x-5x, respectively) with insets of DLS size distributions. X- and y- axes correspond to that of (B).

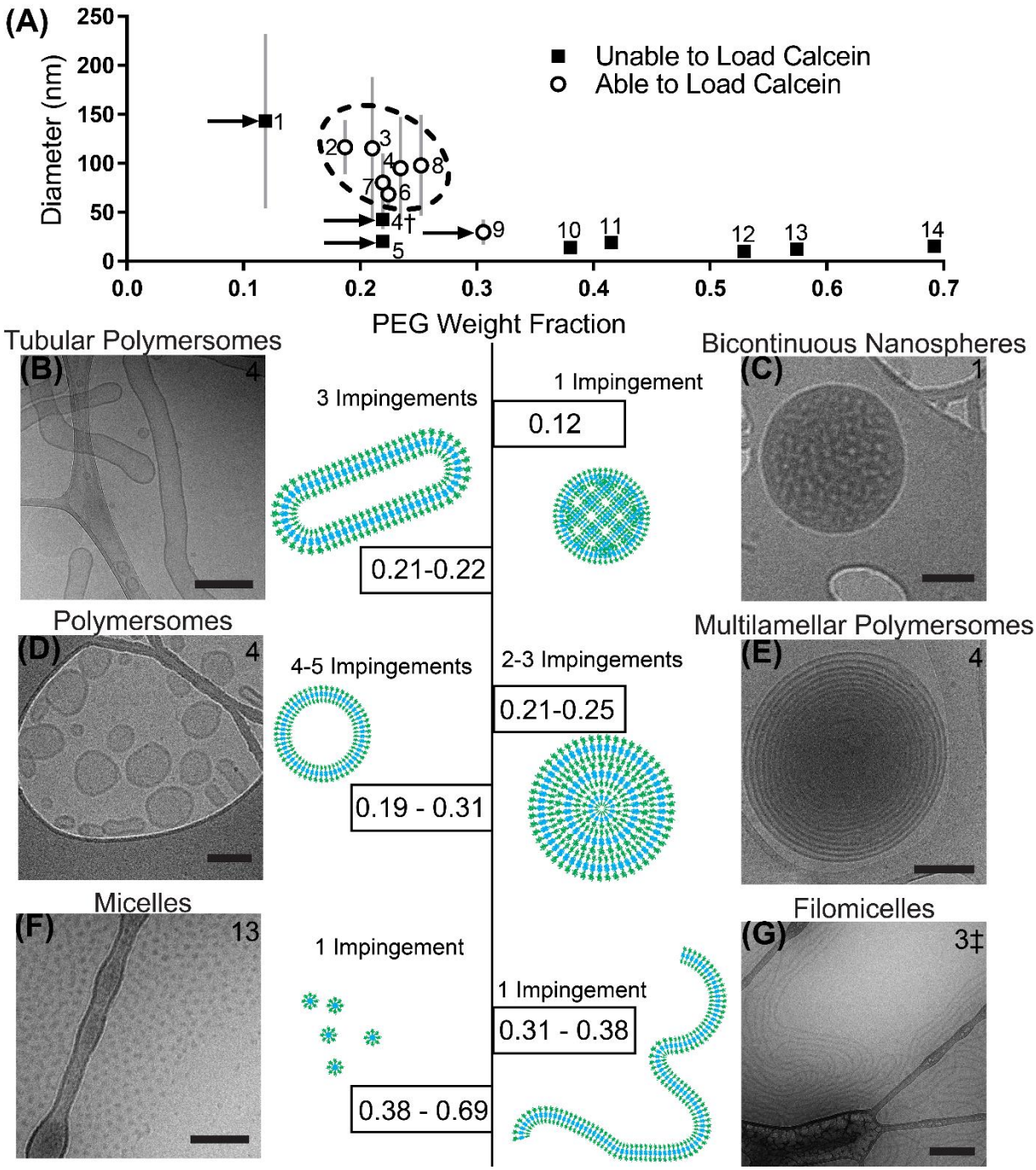

Fig. 3. Relationship between PEG weight fraction and morphology. (A) Diameter of nanostructures formed via FNP from PEG-*bl*-PPS copolymers of varying block lengths. Error bars represent the standard deviation of the nanostructure populations (PDI x Mean Diameter). Dotted area represents polymersome-forming samples. Arrows point out samples of note. †Sample formed using DMF as the organic solvent, rather than THF. ‡Sample formed using water instead of 1xPBS. (B-G) Weight fractions of PEG responsible for forming specific nanostructures via flash nanoprecipitation, paired with cartoon and representative cryoTEM images. All scale bars = 100 nm, with the exception of scale bars within (B) and (E), which are 300 nm. Sample number is listed in the upper corner of each cryoTEM image, and the number of impingements used is listed for each morphology. See Table 1 for details of copolymers and Fig. S5 for low magnification images.

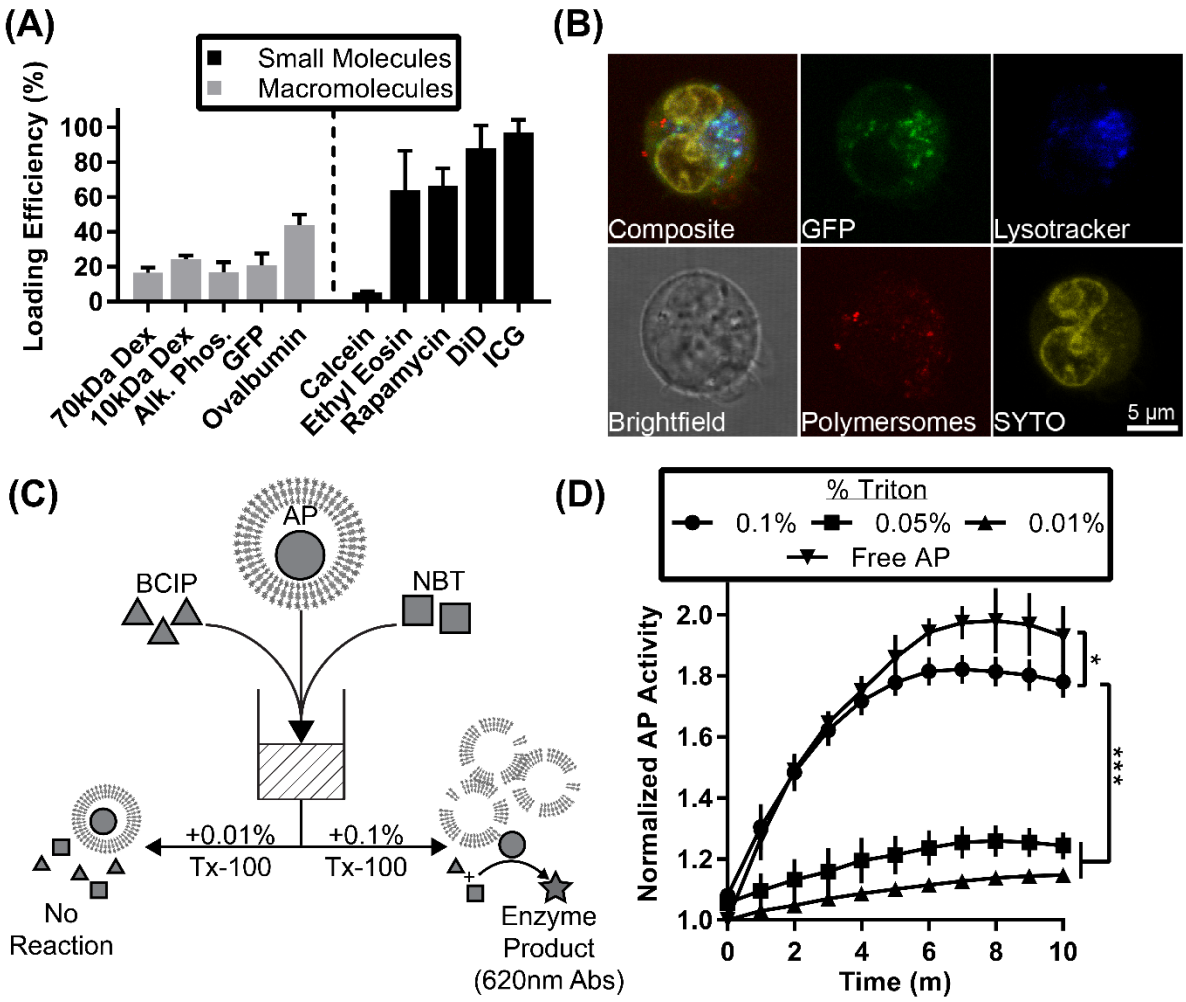

Fig. 4. Loading of polymersomes with small molecules and macromolecules. (A) Loading efficiency of small molecules and macromolecules. (B) Live-cell confocal microscopy image of polymersome uptake and delivery of GFP in a bone marrow-derived dendritic cell. Polymersomes were loaded with the hydrophobic ethyl eosin (red) and hydrophilic GFP (green). Cells were additionally stained with SYTO 61 (yellow) and lysotracker (blue). Scale bar = 5 microns. (C) Graphical representation of experimental setup. Alkaline phosphatase (AP) is represented by circles, BCIP by triangles, and NBT by squares. The product of the enzymatic reaction, formazan, absorbs strongly at 620 nm and is represented by a star. (D) Time-course of enzyme activity assay. Y-axis represents fold increase over original absorbance reading. Error bars represent standard deviation, n = 4. Statistical significance determined by 2-way ANOVA, * $p<0.05$ and *** $p<0.001$.

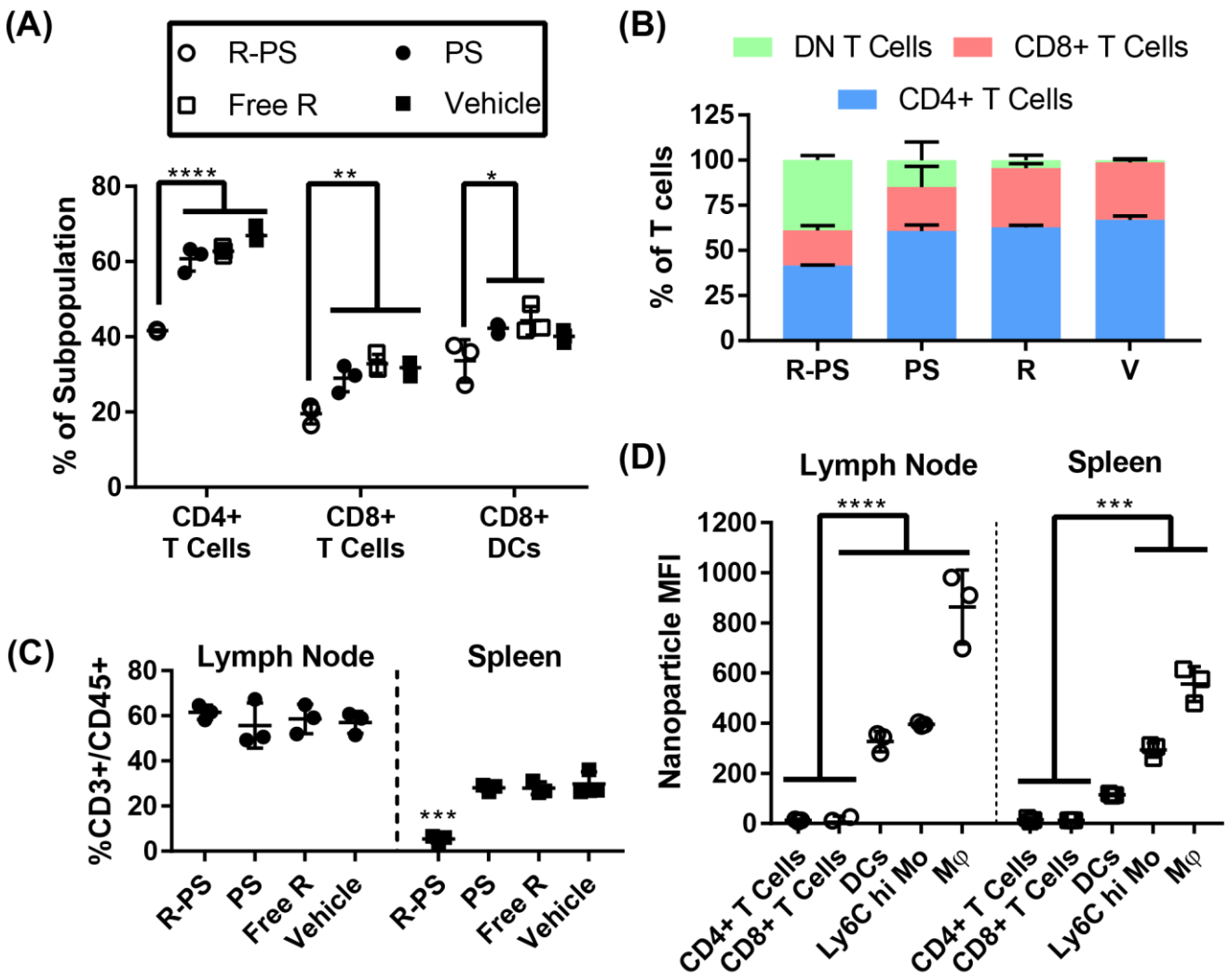

Fig. 5. *In vivo* delivery of theranostic rapamycin/DiD-loaded polymersomes formed by flash nanoprecipitation. (A) Percentage of CD8+ T cells (CD45+ CD3+ CD4- CD8+) and CD4+ T cells (CD45+ CD3+ CD4+ CD8-) within the total T cell population (CD45+ CD3+) and percentage of CD8+ DCs (CD11c+ I-A/I-E+ CD8+) within the total DC (CD11c+) population. Treatment groups were rapamycin polymersomes (R-PS), free rapamycin, blank polymersomes, and vehicle (PBS). (B) T cell subpopulations as a percent of total T cell population for all four treatment groups. (C) T cells in the spleen and lymph nodes, as a percentage of CD45+ cells. (D) Median fluorescence intensity of the polymersome channel for selected cell populations in the spleen and lymph nodes of mice administered rapamycin/DiD-loaded polymersomes. N=3, statistical significance determined by Tukey's multiple comparisons test, * $p < 0.05$, ** $p < 0.01$, ***$p < 0.001$, ****$p < 0.0001$.

#	PEG DoP	PPS DoP	f_{PEG}	End Capping	Com/Aqu Solv	D (nm)	PDI	Morphology
1	17	75	0.119	Thiol	THF/PBS	143.13	0.62	**BN,** M, P
2	17	44	0.187	Benzyl	THF/PBS	116.53	0.24	**P**
3	17	38	0.21	Thiol	THF/PBS	115.29	0.63	**P,** MLP***, TP***
3‡					THF/Water	N/A	N/A	**FM**
4	17	36	0.219	Thiol	THF/PBS	80.51	0.37	**P,** MLP***, TP***
4†					DMF/PBS	41.53	0.31	**M,** P**
5	45	96	0.219	Benzyl	THF/PBS	20.54	0.25	**M**
6	17	35	0.224	Pyridyl Sulfide	THF/PBS	68.58	0.22	**P,** MLP***, TP***
7	17	33	0.235	Thiol	THF/PBS	95.06	0.55	**P,** MLP*****
8	17	30	0.252	Thiol	THF/PBS	97.96	0.52	**P,** MLP*****
9	17	23	0.305	Thiol	THF/PBS	29.78	0.43	**M,** P, FM
10	45	44	0.38	Benzyl	THF/PBS	14.28	0.33	**M,** FM
11	45	38	0.415	Phthalimide	THF/PBS	19.03	0.29	**M**
12	45	24	0.529	Benzyl	THF/PBS	10.13	0.38	**M**
13	45	20	0.574	Benzyl	THF/PBS	12.75	0.3	**M**
14	45	12	0.692	Benzyl	THF/PBS	15.43	0.43	**M**

Table 1. Relationship between PEG weight fraction (f_{PEG}) and morphology. Com/Aq Solv = Common/Aqueous Solvents used during the impingement process. M = Micelles, FM = Filomicelles, BN = Bicontinuous Nanospheres, P = Polymersomes, MLP = Multilamellar Polymersomes, TP = Tubular Polymersomes. Predominant population(s) shown in **bold**. *Population only found after multiple impingements. **Very rare population. DLS diameter and polydispersity data not available for samples predominantly composed of filomicelles, i.e. sample 3‡.

Dual Loaded Cargoes	Hydrophilic Loading (%)	Hydrophobic Loading (%)	logP Values
TMR-Dextran 70kDa, ICG	16.60 ± 2.98	97.12 ± 7.04	N/A, 9.056
Alkaline Phosphatase, Ethyl Eosin	19.00 ± 5.62	64.91 ± 5.42	N/A, 7.497
Calcein, Ethyl Eosin	5.06 ± 1.66	52.02 ± 2.65	1.608, 7.497
Calcein, DiI	2.54 ± 2.17	103.47 ± 12.11	1.608, 18.824
GFP, Ethyl Eosin	20.85 ± 6.74	63.71 ± 8.42	N/A, 7.497
Rapamycin, DiD	N/A	65.59 ± 7.21 87.88 ± 13.11	6.181, 19.38

Table 2. Loading efficiency for dual-loading by flash nanoprecipitation. All samples fabricated in triplicate. LogP values given when available.

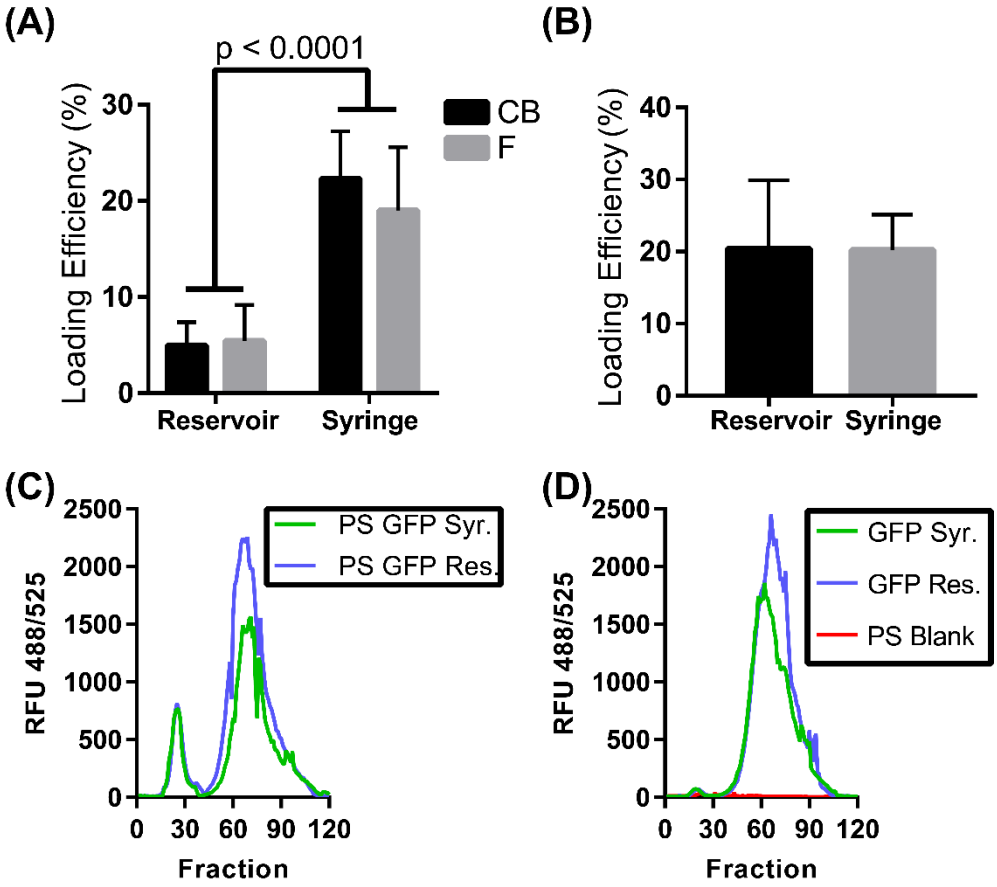

Fig. S1. Efficiency of loading via syringe or reservoir. (A) Loading efficiency of fluorescently-labeled 10kDa dextrans (CB = cascade blue, F=fluorescein). Error bars represent standard deviation, n = 6. (B) Loading efficiency of GFP when loaded via either syringe or reservoir. Error bars represent standard deviation, n = 3. (C) Fluorescence of sepharose CL-6B column separated GFP-loaded polymersomes loaded *via* syringe or reservoir, 200 µL fractions. (D) Fluorescence of sepharose CL-6B column separated GFP processed *via* FNP through the syringe or reservoir without PEG-*bl*-PPS copolymer, as a control. Included is a trace of blank polymersomes, for reference.

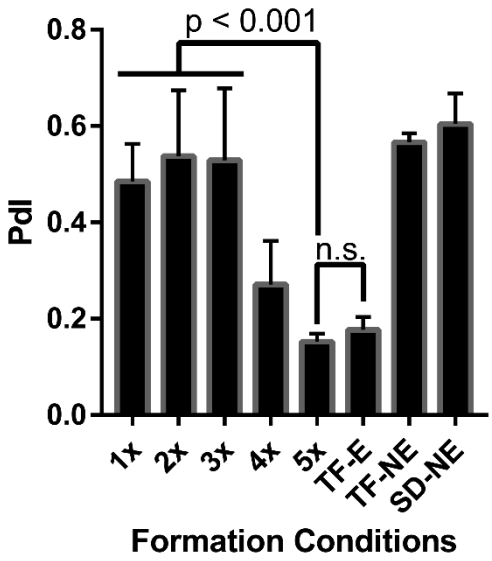

Fig. S2. DLS mean polydispersity (PdI) of polymersomes formed after multiple impingements (1x-5x), or formed by thin film (TF) or solvent dispersion (SD) with (E) or without (NE) extrusion. Error bars are standard error, n = 5.

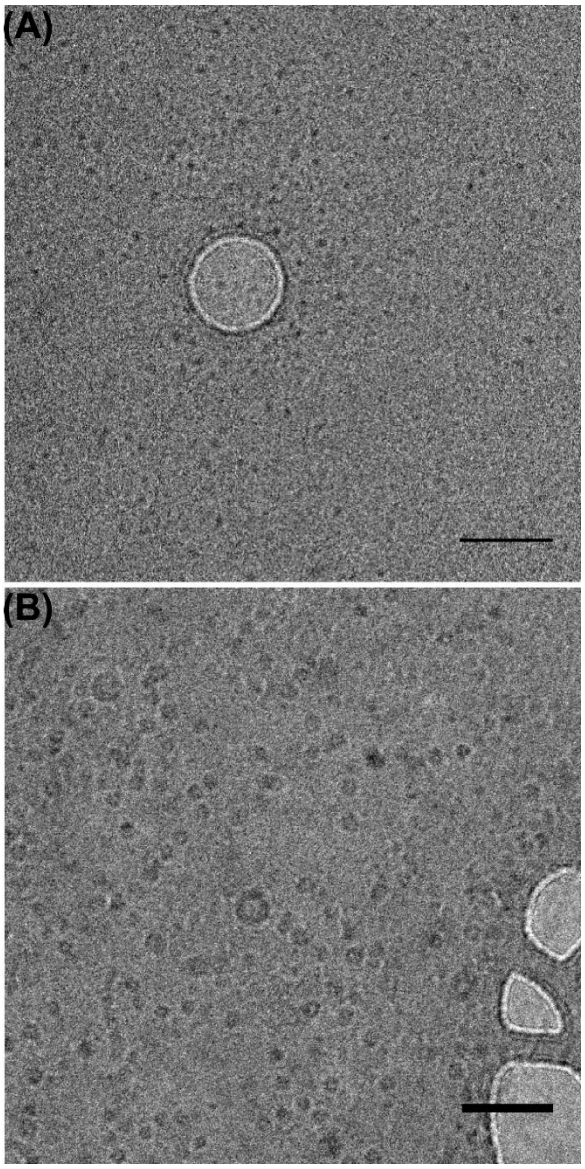

Fig. S3. CryoTEM images of copolymers 5 and 9. (A) Micelles were formed by copolymer 5. (B) Micelles and occasional polymersomes were formed by copolymer 9. All scale bars represent 100 nm.

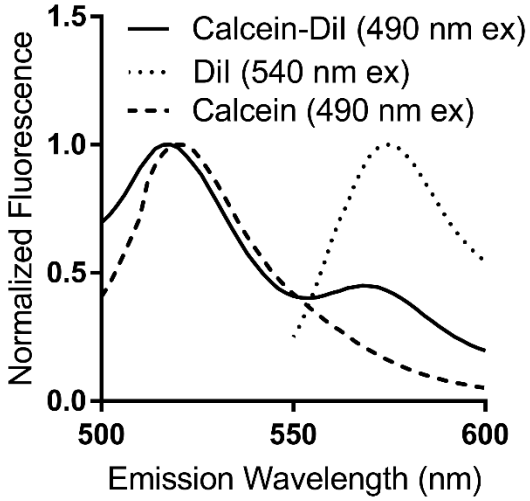

Fig. S4. Emission spectra of calcein-DiI dual loaded polymersomes. Calcein-DiI polymersome emission (490 nm excitation) is represented by the solid black line. Calcein and DiI emission spectra are included in the plot for reference.

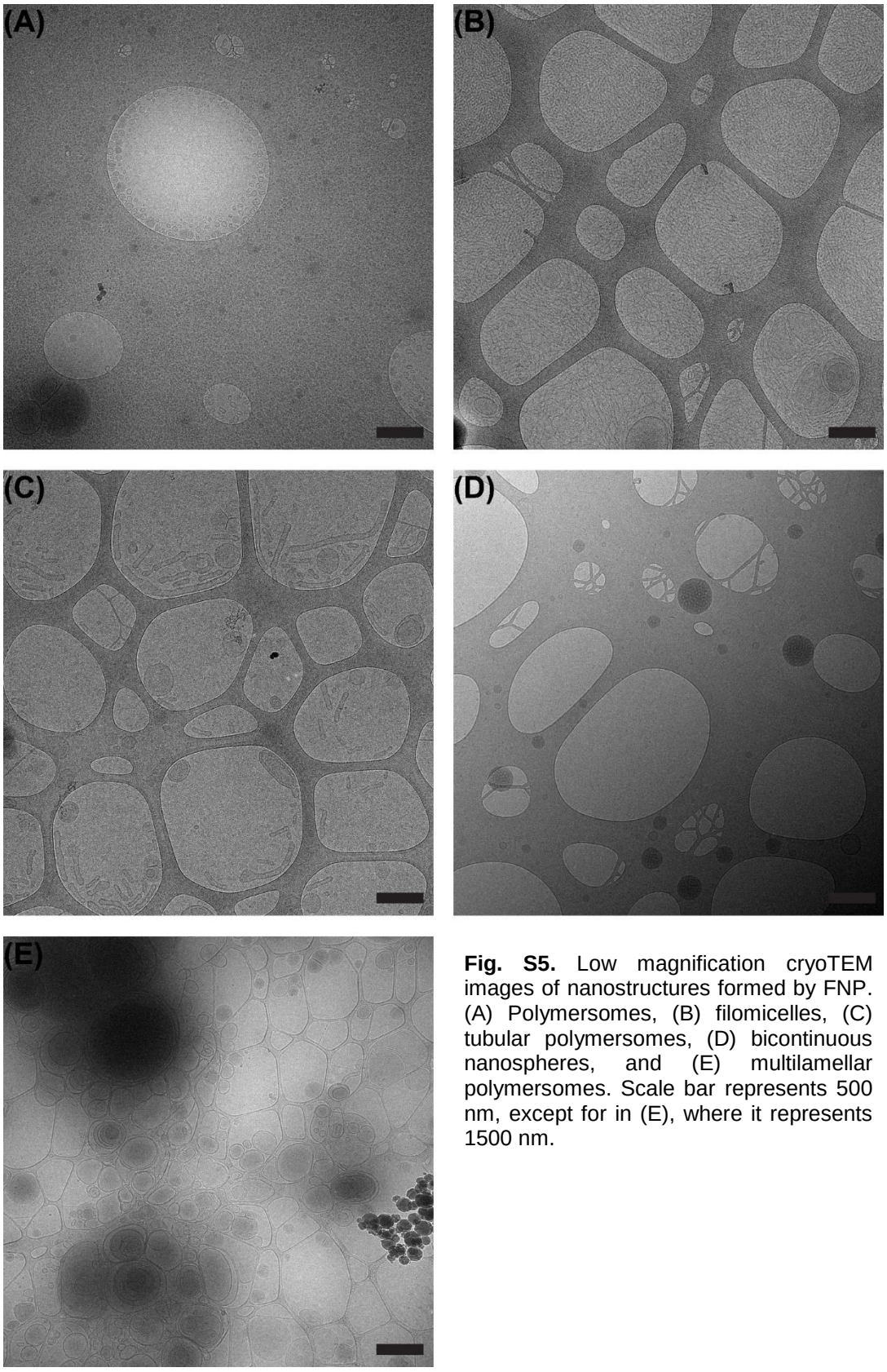

Fig. S5. Low magnification cryoTEM images of nanostructures formed by FNP. (A) Polymersomes, (B) filomicelles, (C) tubular polymersomes, (D) bicontinuous nanospheres, and (E) multilamellar polymersomes. Scale bar represents 500 nm, except for in (E), where it represents 1500 nm.

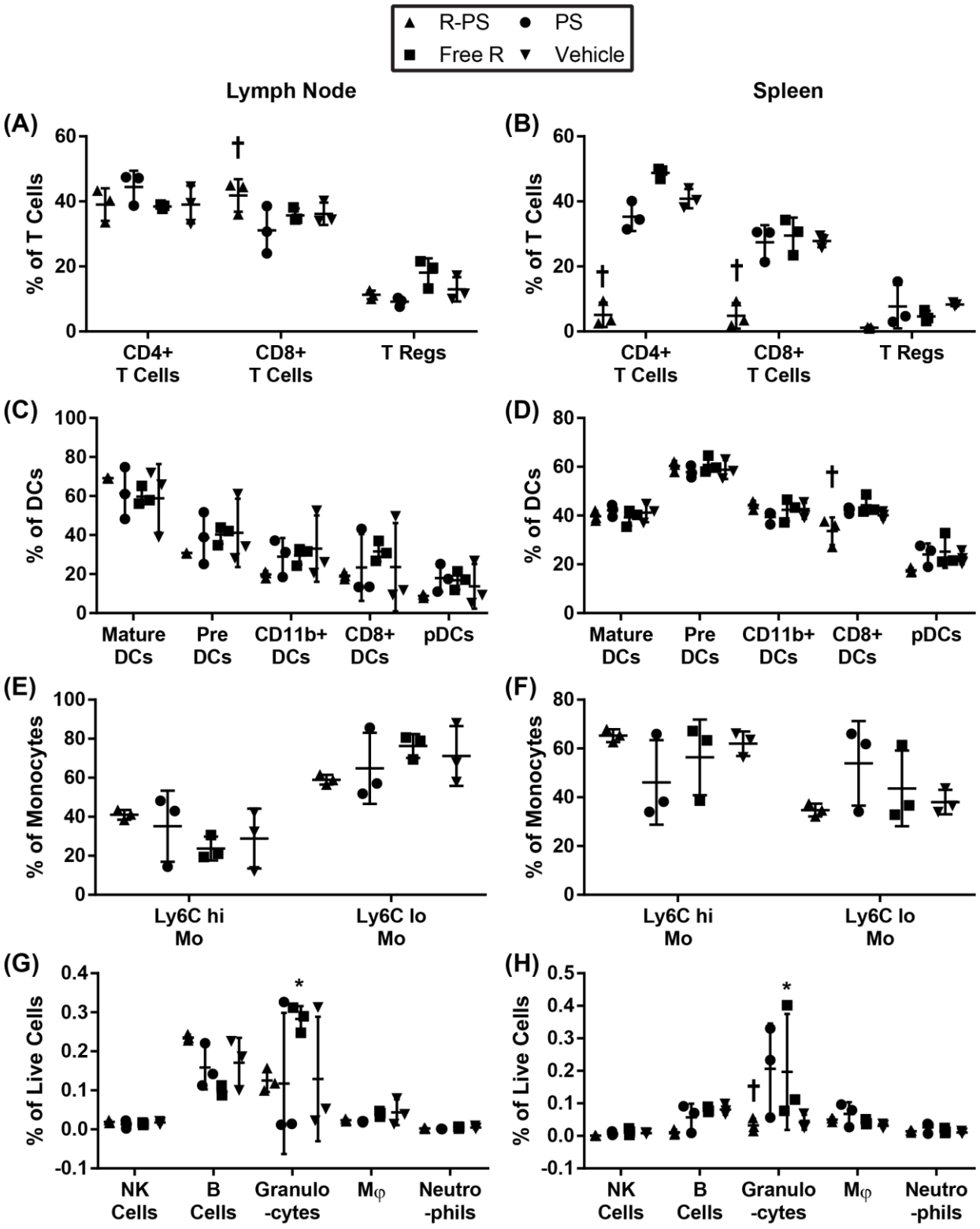

Fig. S6. Percentages of total live cells in the lymph nodes (A, C, E, G) and spleen (B, D, F, H) that are T cells, dendritic cells (DCs), plasmacytoid dendritic cells monocytes (Mo), B cells, granulocytes, macrophages (Mφ), and neutrophils. † indicates rapamycin polymersome treated populations that were significantly altered compared to blank polymersomes. * indicates free rapamycin treated populations that were significantly altered compared to vehicle.

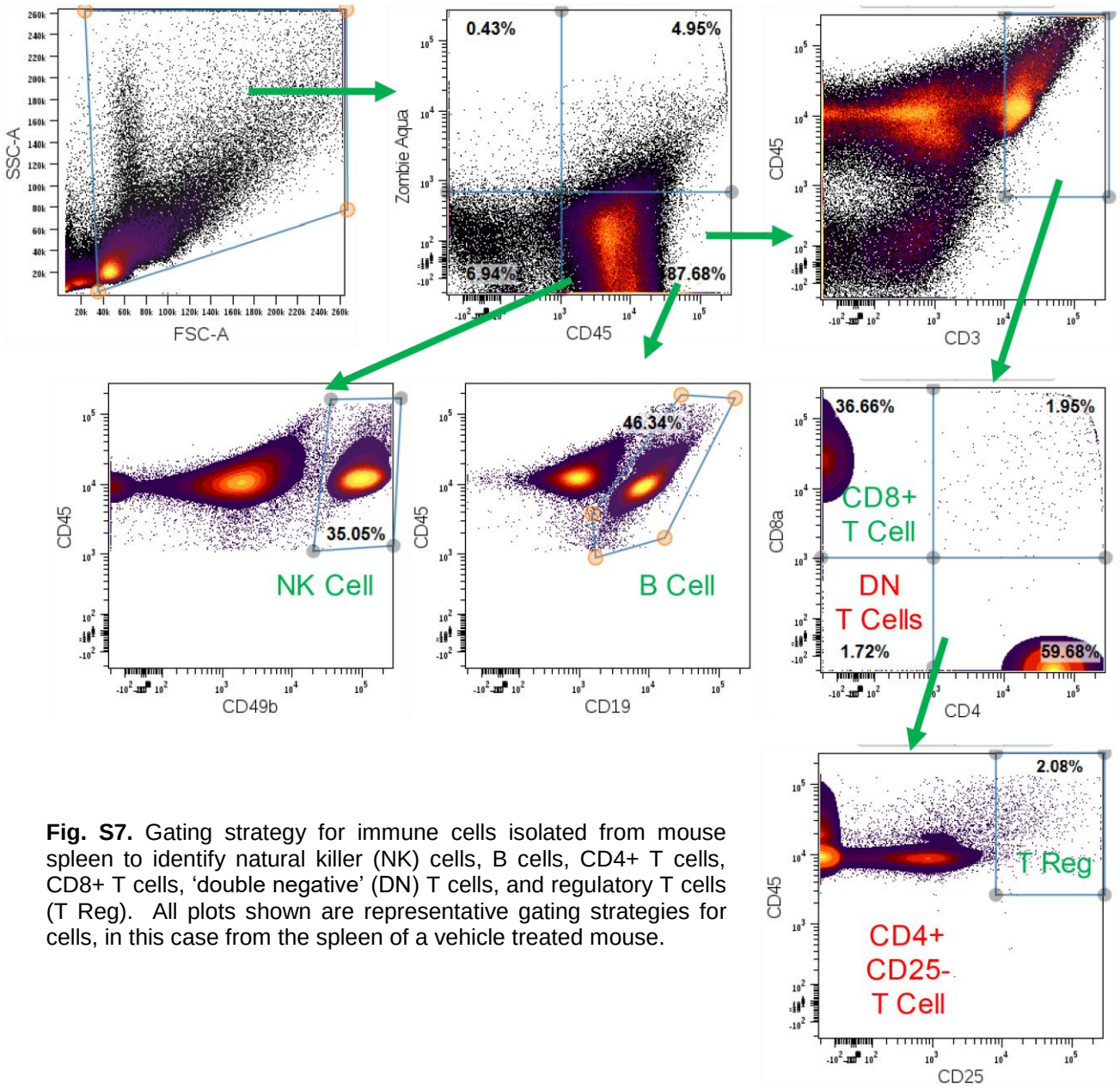

Fig. S7. Gating strategy for immune cells isolated from mouse spleen to identify natural killer (NK) cells, B cells, CD4+ T cells, CD8+ T cells, 'double negative' (DN) T cells, and regulatory T cells (T Reg). All plots shown are representative gating strategies for cells, in this case from the spleen of a vehicle treated mouse.

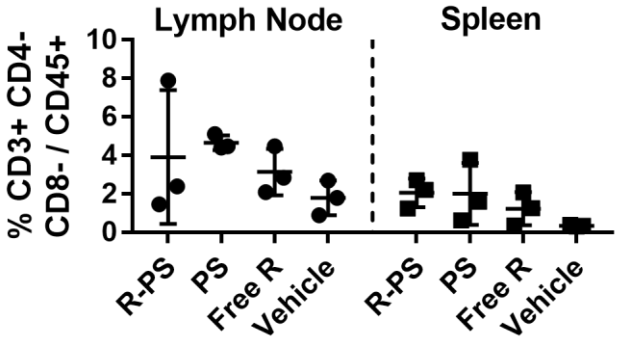

Fig. S8. Percentage of DN T cells within the CD45+ cell population in the lymph nodes and spleen. N = 3.